Advances in Aircraft and Spacecraft Science, *Vol. 9, No. 2 (2022) 103-117*
https://doi.org/10.12989/aas.2022.9.2.103

Variable camber morphing wing mechanism using deployable scissor structure: Design, analysis and manufacturing

Yeeryung Choi[1a] and Gun Jin Yun*[2]

[1]*Department of Aerospace Engineering, Seoul National University, Seoul, 08826, South Korea*
[2]*Institute of Advanced Aerospace Technology, Seoul National University, Seoul, 08826, South Korea*

(Received August 25, 2021, Revised January 24, 2022, Accepted February 5, 2022)

Abstract. In this paper, a novel morphing mechanism using a deployable scissor structure was proposed for a variable camber morphing wing. The mechanism was designed through the optimization process so that the rib can form the target airfoils with different cambers. Lastly, the morphing wing was manufactured and its performance was successfully evaluated. The mechanism of the morphing wing rib was realized by a set of deployable scissor structure that can form diverse curvatures. This characteristic of the structure allows the mechanism to vary the camber that refers to the airfoil's curvature. The mechanism is not restrictive in defining the target shapes, allowing various airfoils and overall morphing wing shape to be implemented.

Keywords: aircraft; morphing wing; optimization; variable compliant camber wing

1. Introduction

A morphing wing refers to the wing that changes its geometry. The morphing wings have been actively researched because it can reduce fuel consumptions by simplifying control surfaces of the wing. Since the fixed-shape wings respond to the flight conditions using additional devices such as flaps, elevators, ailerons, slats etc., these devices create a discontinuous surface. However, in the case of the morphing wing, the wing's shape can change without discontinuous surface. Thus, as compared to the conventional wing, the morphing wing can have a wider operating range of efficient performance under a given flight environment (Barbarino *et al.* 2011, Wlezien *et al.* 1998, Sofla *et al.* 2010).

Morphing wings are classified into planform alteration, out-of-plane alteration, and airfoil adjustment according to the geometry to be deformed (Barbarino *et al.* 2011). Wings with variations in chord, span, and sweep belong to planform alteration wings (Ajaj *et al.* 2016, Ajaj *et al.* 2013, de Marmier and Wereley 2003, Mestrinho *et al.* 2011, Prabhakar *et al.* 2015, Tarabi *et al.* 2016, Vocke III *et al.* 2011). Prabhakar *et al*. designed and constructed a variable-span and variable-sweep morphing wing. They also analyzed the morphing wing's longitudinal dynamic behavior with varying rates of change (Prabhakar *et al.* 2015). Morphing wings that form twist, dihedral/gull, and spanwise bending are out-of-plane alterations (Abdulrahim 2005, Abdulrahim and Lind 2004,

*Corresponding author, Professor, E-mail: gunjin.yun@snu.ac.kr
[a]Ph.D. Student, E-mail: marchx31@snu.ac.kr

http://www.techno-press.org/?journal=aas&subpage=7 ISSN: 2287-528X (Print), 2287-5271 (Online)

Bourdin *et al.* 2008, Cuji and Garcia 2008, Detrick and Washington 2007, Elzey *et al.* 2003, Majji *et al.* 2007, Raither *et al.* 2013, Vos *et al.* 2010). Abdulrahim *et al*. presented a bio-inspired morphing method and applied it successfully to a 24-inch aircraft (Abdulrahim 2005). Majji *et al*. proposed a new twist morphing wing with an elastomeric skin (Majji *et al.* 2007). The wing's aerodynamic performance was tested in a wind tunnel at a low speed. Among the morphing wings implementing the airfoil adjustment, a variable camber morphing wing is defined as a morphing wing with airfoil camber altered. The camber implies the curvature of the airfoil, and diverse methods have been devised to alter the camber. To change the wing's curvature, the wing is deformed partially or entirely. The camber geometry is changed by bending a partial part such as the leading edge and trailing edge part or deflecting the airfoil's entire shape (Dale *et al.* 2013, Zhang *et al.* 2021, Seow *et al.* 2008, Yokozeki *et al.* 2014a, Yokozeki *et al.* 2014b, Dimino *et al.* 2017, Marques *et al.* 2009, Monner *et al.* 2009, Kimaru and Bouferrouk 2017, Joo *et al.* 2015, Marks *et al.* 2015, Rivero *et al.* 2018, Rivero *et al.* 2017). Yokozeki *et al*. applied a corrugated structure to the variable camber morphing wing controlled by wires (Yokozeki *et al.* 2014a). They demonstrated the wing's performance in the wind tunnel test under different air speeds and the angle of attack (Yokozeki *et al.* 2014b). Joo *et al*. designed and fabricated a variable camber compliant wing (Joo *et al.* 2015). Their wing has a smooth deformation of the camber. The wing was experimented to examine changing camber at a low flight speed and DIC (Digital Image Correlation) was used to indicate the wing's deformation under aerodynamic load (Marks *et al.* 2015). Also, Pagani *et al*. researched the use of the DIC technique measuring the composite wing's displacement and strain (Pagani *et al.* 2019).

There are several methods to deform the wing's shape such as using shape memory material, applying an internal mechanism, etc. Among these methods, many studies have been conducted to change the wing's configurations by using structural characteristics that allow deformations. One of these studies, Finistauri and Xi used a truss structure as a mechanism for a morphing wing to deform the geometry (Finistauri and Xi 2009). The members that comprise this truss structure are replaced with prismatic joints to morph as an individual or simultaneous wing sweep, dihedral twist and span. In another case, Andersen *et al*. applied four-bar linkages to a morphing wing changing the sweep angle. Also, they implemented flutter analyses on the wing for aerodynamic models with five configurations (Andersen *et al.* 2007). In this study, the deployable structure was applied to the internal mechanism and the wing is deformed due to this structure's characteristics. A deployable structure can be transformed in various shapes, sizes and volumes. It takes a predetermined geometry deforming through known paths during deployment and retraction (Fenci and Currie 2017). Among the various deployable structures (De Temmerman 2007), the deployable scissor structure is composed of straight bars and revolute joints, and the structure's shape is determined by the length of the bars, the angle between the bars, and the hinge position (Roovers and De Temmerman 2017, Langbecker 1999, Zhao *et al.* 2009). In other words, given that the dimensions and their relative angles are optimized, the targeted shape can be formed by the structure.

In this paper, a novel variable camber morphing wing with a unique internal mechanism was proposed by applying the deployable scissor structures. This internal mechanism is designed using the deployable structure to form various airfoil shapes through an optimization process to form the targeted airfoils with various cambers. The target airfoil shapes are set to NACA 4-digit airfoil shapes (i.e., NACA2410, NACA3410, NACA4410, NACA5410, NACA6410, NACA7410, NACA8410) that have different cambers but the same length of the chord line. The mechanism was optimized to form the target shapes, and therefore each of the ribs can accurately form the intended shapes. In operability, an actuator is embedded for a rib. Therefore, the rib can form the shape

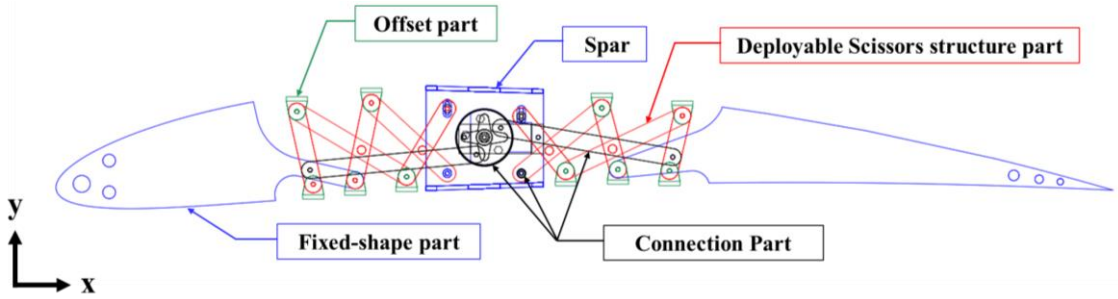

Fig. 1 Design and part classification of the variable camber morphing wing rib

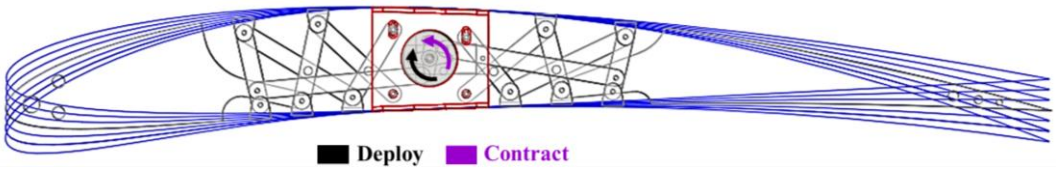

Fig. 2 Spar location with the targeted airfoil shapes

independently, and the wing can perform a twisted morphing wing. Lastly, the morphing wing was manufactured and confirmed to exhibit the targeted shapes with varying airfoil's camber.

2. Design of ınternal mechanism for variable-camber Morphing wing

2.1 Applications of deployable scissor structure

The targeted airfoil shapes with varying cambers are formed by applying the deployable scissor structure to the morphing wing of the aircrafts. Fig. 1 shows the internal mechanism consisting of deployable scissor structure parts, fixed shaped parts, connection parts, offset parts, and an actuator. Among these, the deployable scissor structure part determines the overall shape. The fixed-shape parts are composed of a spar, a leading-edge part, and a trailing-edge part. The spar is fixed in both position and shape. However, other fixed parts move their positions following the deployable scissor structure part. The actuator is located inside the spar, and the connection parts connect the deployable scissor structure with the leading and trailing edge parts. The offset parts are connected to the bars with revolute joints. The offset parts serve to make the contact surface with the skin covering the whole morphing wing. The skin should be contemplated as it can affect the wing's operability. However, this paper focused on the morphing mechanism and the skin will be researched in the future. The fixed leading and trailing edge parts are derived from NACA 5410, having the intermediate camber value of the target airfoils. All target shapes are designed to have the same maximum thickness and maximum camber position. Since the spar has a fixed position, there is a difference between the spar and the target shapes. However, this difference in coordinates is less than 1.5% of the maximum thickness. The blue lines in Fig. 2 represent the target airfoils, and the spar is marked with a red line. Fig. 3 shows the connection parts that transmit the driving force from the actuator to the fixed-shape parts and allow the parts to link together. The rotating actuator provides power so that the rib can independently implement the desired shape. Also, actuator lines

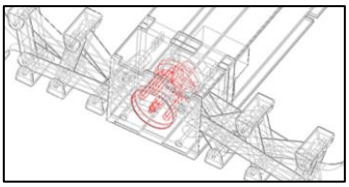

(a) Rotating part fixed with the actuator

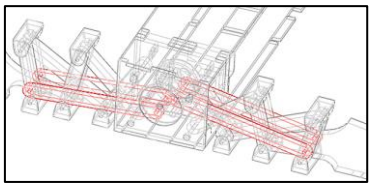

(b) Actuator lines

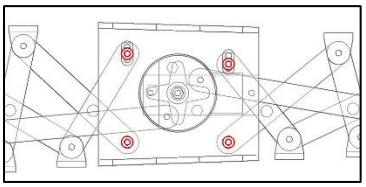

(c) Bars between the spar and deployable structure parts

Fig. 3 Connection parts

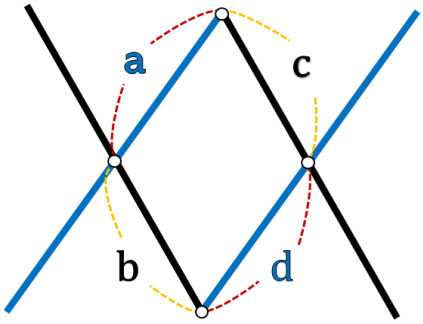

Fig. 4 A basic unit of the deployable scissor structure

limit the structure's movement, transmit the driving force to the deployable scissor structure and increase the stability of the structures.

2.2 Mathematical formulation for the ınternal mechanism

Since the deployable scissor structure plays a significant part in altering the shape, it is critical to understand how the structure's shape is determined by changing its lengths and angles. A basic unit of the deployable scissor structure consists of two straight bars and a revolute joint connecting them, as shown in Fig. 4. A mathematical model is formulated based on deployability constraint in Eq. (1) that should be satisfied to deploy the structure (De Temmerman 2007).

$$a + b = c + d \tag{1}$$

where a,b,c, and d are the length of the basic unit of the deployable scissor structure in Fig. 4.

The mathematical model is devised for how arbitrary dimensions satisfying this condition form the structural shape. Fig. 1 shows the coordinate system, where the x-axis direction refers to the chordwise direction. Based on the spar, each of the deployable scissor structure parts connected to the leading edge part and the trailing edge part is designed in the same way, and these parts have the same number of units. In Fig. 5, the deployable scissor structure connected to the trailing edge part is linked to the spar with two bars. The upper bar belonging to the connection bars moves only on the y-axis and its location is set to Point ②. The position of the lower bar fixed to the spar is set to Point ①. These points have an identical x-coordinate value and are on the same plane. The actuator's movement determines Point ②, and Point ① has the coordinate with fixed and given values. In Fig. 5, the deployable scissor structure jointing the trailing edge part is indicated, and the hinge point of the first unit from the spar is set to Point ③. The triangle ①-②-③ in Fig. 5 has the

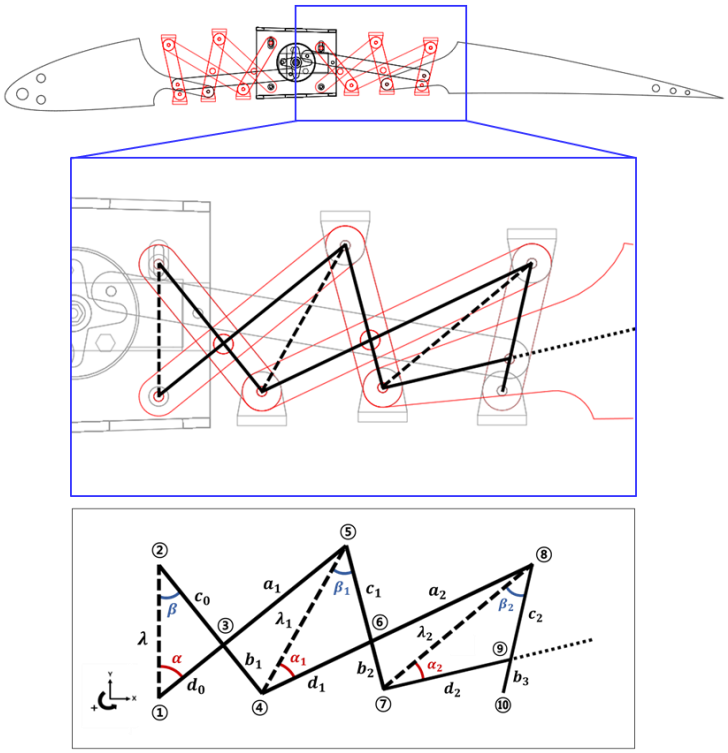

Fig. 5 Schematics of deployable structure parts composed of scissor units on the trailing edge side

length λ between Points ① and ②, the length d_0 between Points ① and ③ and the length c_0 between Points ② and ③. The angles of the triangle designated α and β are determined by the cosine rule applied to the triangle ①-②-③ as in Eq. (2) and Eq. (3). Consider a vector $\vec{V}_{1-3}$ from Point ① to Point ③. The unit vector $\vec{v}_{1-2}$ from Point ① to Point ② is (0,1,0). If the unit vector $\vec{v}_{1-2}$ is rotated clockwise by the angle α, the unit vector $\vec{v}_{1-3}$ from Point ① to Point ③ can be obtained. If the magnitude d_0 is given, the vector $\vec{V}_{1-3}$ can be obtained by Eq. (4), Eq. (5), Eq. (6), and Eq. (7).

$$\alpha = cos^{-1}\left(\frac{\lambda^2 + {d_0}^2 - {c_0}^2}{2\lambda d_0}\right) \tag{2}$$

$$\beta = cos^{-1}\left(\frac{\lambda^2 + {c_0}^2 - {d_0}^2}{2\lambda c_0}\right) \tag{3}$$

$$\vec{v}_{1-2} = \begin{bmatrix} x_2 \\ y_2 \\ z_2 \end{bmatrix} - \begin{bmatrix} x_1 \\ y_1 \\ z_1 \end{bmatrix} \tag{4}$$

$$\vec{v}_{1-2} = \frac{\vec{v}_{1-2}}{\|\vec{v}_{1-2}\|} = \begin{bmatrix} 0 \\ 1 \\ 0 \end{bmatrix} \tag{5}$$

$$A_{rot} = \begin{bmatrix} cos(-\alpha) & -sin(-\alpha) & 0 \\ sin(-\alpha) & cos(-\alpha) & 0 \\ 0 & 0 & 1 \end{bmatrix} \tag{6}$$

$$\vec{V}_{1-3} = d_0 * A_{rot} * \vec{v}_{1-2} \tag{7}$$

$$\vec{v}_{2-1} = \frac{\vec{V}_{2-1}}{\|\vec{V}_{2-1}\|} = \begin{bmatrix} 0 \\ -1 \\ 0 \end{bmatrix} \tag{8}$$

$$B_{rot} = \begin{bmatrix} cos(\beta) & -sin(\beta) & 0 \\ sin(\beta) & cos(\beta) & 0 \\ 0 & 0 & 1 \end{bmatrix} \tag{9}$$

$$\vec{V}_{2-3} = c_0 * B_{rot} * \vec{v}_{2-1} \tag{10}$$

$$\vec{V}_{1-5} = (d_0 + a_1) * A_{rot} * \vec{v}_{1-2} \tag{11}$$

$$\vec{V}_{2-4} = (c_0 + b_1) * B_{rot} * \vec{v}_{2-1} \tag{12}$$

In the same way, by Eq. (8), Eq. (9), and Eq. (10), the unit vector $\vec{v}_{2-1}$ is rotated counterclockwise by the angle β to find the unit vector $\vec{v}_{2-3}$. If the length c_0 is given to the rotated unit vector $\vec{v}_{2-3}$, the vector $\vec{V}_{2-3}$ can be obtained. Consequently, the coordinate of Point ③ is obtained using the coordinates of Point ① and Point ②. Using the vectors and the members' lengths with arbitrary values, the first unit, and the second unit's points can be represented by the dimensions and obtained through Eq. (11) and Eq. (12). Additionally, the unit vector $\vec{v}_{1-3}$ is the same as the unit vector $\vec{v}_{1-5}$. The unit vector $\vec{v}_{2-3}$ is the same as the unit vector $\vec{v}_{2-4}$. Thus, the coordinates of Point ④ and Point ⑤ shown in Fig. 5 can be obtained by applying the values of Point ① and Point ②.

The relationship between the points can be calculated using same principle and repeatedly applying the method to the deployable scissor units. In other words, the coordinates can be obtained by using arbitrary lengths and the coordinates of the bars linking the spar and the structure.

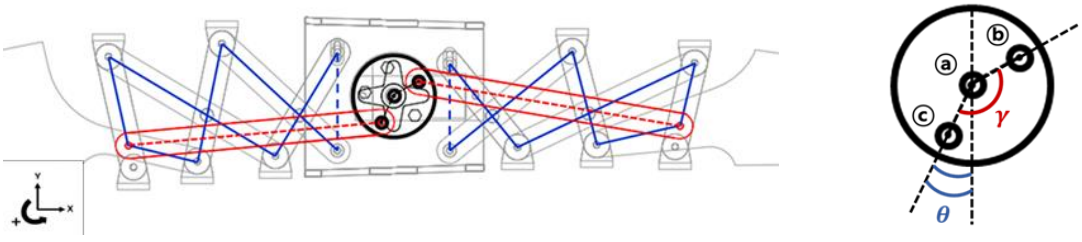

(a) Deployable structure parts and Actuator lines (b) Rotating connection part

Fig. 6 Schematics of connection between the deployable structure and the actuator

Table 1 The input angles for each target airfoil shapes

Airfoil	NACA 2410	NACA 3410	NACA 4410	NACA 5410	NACA 6410	NACA 7410	NACA 8410
Angle θ	7°	13°	19°	25°	31°	39°	49°

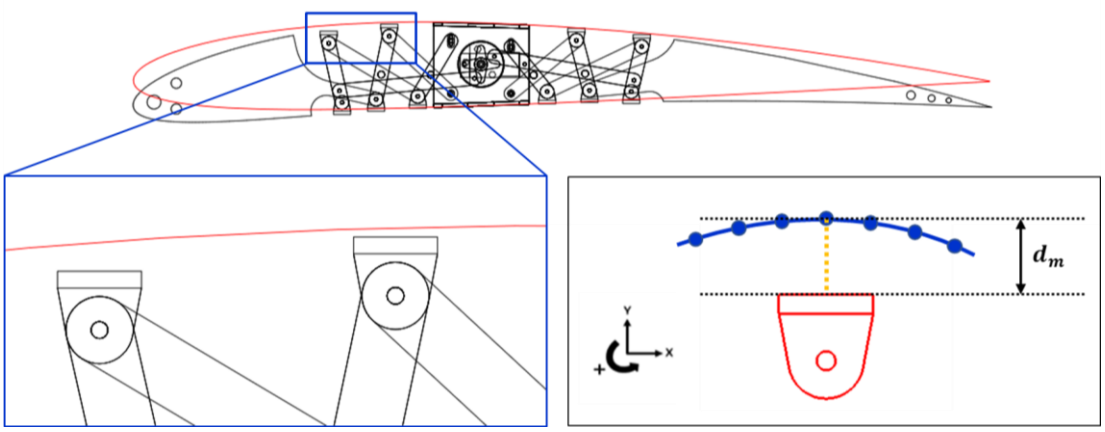

Fig. 7 The difference between the rib's shape and the target airfoil

2.3 Actuation modeling of the internal mechanism

The design variables for the shape are the deployable scissor members' lengths and angles. In this paper, the angles are set to fixed values and lengths to have arbitrary values. In Fig. 6(a), the blue lines indicate deployable scissor structure, the red lines are actuator lines, and the rotating connection part was marked as the black line. As shown in Fig. 6(b), the center point of the rotating connection part is Point ⓐ. At Point ⓑ and Point ⓒ, the rotating part and the actuator lines are connected. The angle γ between the straight line ⓐ-ⓑ and the straight line ⓐ-ⓒ has a fixed value. On the other hand, the angle θ between the vertical line passing through Point ⓐ and the straight line ⓐ-ⓒ varies as the rotating connection part revolves. This angle θ is the control variable. The θ values corresponding to the targeted airfoils are summarized in Table 1.

3. Optimal dimension of the internal mechanism for variable camber Morphing wing

The member lengths are determined by minimizing the difference between the targeted shapes and the airfoil curve that the mechanism makes. The outermost edge of the rib shape is formed by the offset part, the leading and the trailing edge parts. The offset part's coordinates and the targeted coordinates are matched based on the x-coordinate values. The center point of the offset part's surface and its closest point on the airfoil curve are paired, as shown in Fig. 7. The offset parts are connected to the structure by revolute joints. For four cases shown in Fig. 8, the distance is calculated as shown in Fig. 7. Among the four cases, the smallest distance d_m was measured as the coordinate difference in Eq. (13).

$$d_m = \sqrt{(x_{ra} - x_{sc})_m{}^2 + (y_{ra} - y_{sc})_m{}^2 + (z_{ra} - z_{sc})_m{}^2} \tag{13}$$

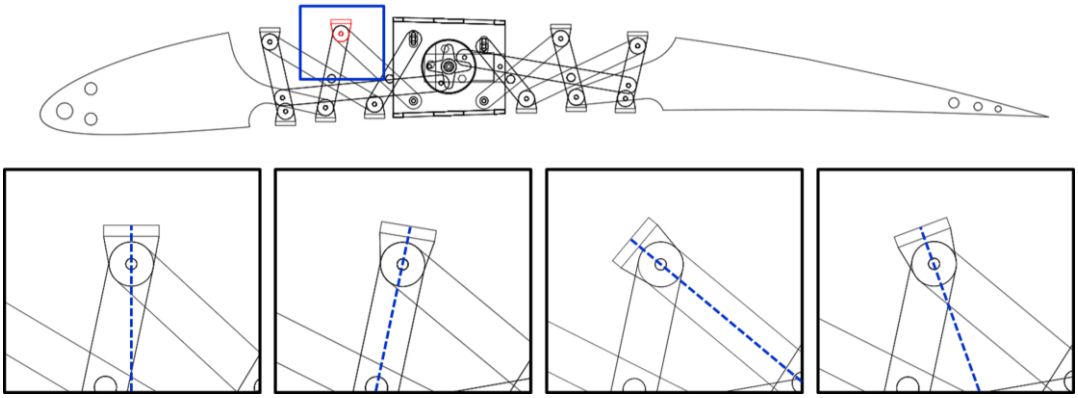

Fig. 8 Four cases for offset part rotation angles

where $[\mathbf{x_{ra}}, \boldsymbol{y_{ra}}, \boldsymbol{z_{ra}}]_{\boldsymbol{m}}$ $(\mathbf{m} = \mathbf{1}, \mathbf{2}, \ldots)$ is the targeted airfoil coordinate and $[\mathbf{x_{sc}}, \boldsymbol{y_{sc}}, \boldsymbol{z_{sc}}]_{\boldsymbol{m}}$ $(\mathbf{m} = \mathbf{1}, \mathbf{2}, \ldots)$ is the offset part surface coordinate. $\mathbf{S_a}$ is the sum of the differences as follows

$$S_a = \sum_{m=1}^{N} d_m \tag{14}$$

where N is the number of points along the airfoil curves. The objective function $\mathbf{T_{ta}}$ is the sum of all $\mathbf{S_a}$ values.

$$T_{ta} = \sum_{i=1}^{M} S_{ai} \tag{15}$$

where M is the number of the NACA airfoils considered in this paper. The optimization process determines the lengths of the deployable scissor structures by minimizing the objective function. Constraints considered include the deployability constraint, the number of scissor units, the actuator lines' lengths and locations. The algorithm is implemented by the MATLAB 'fmincon'. Furthermore, if the objective function change is less than 10^{-7}, the algorithm is terminated. Fig. 9 shows changes of the objective function during the optimization process. The final T_{ta} was 13.56 mm.

3.1 Morphing wing design model and simulation

The rib model was designed by applying length dimensions obtained from the optimization process. The design goal was to make each rib deform to the airfoil independently maintaining the chord length. Since the deployable structure part deploys and contracts as the actuator rotates, the morphing ribs' chord length cannot maintain the same value during deformation. However, the maximum difference is less than 1% of the design chord length. Therefore, the difference is negligible.

The camber morphing wing in Fig. 10 consists of fifteen ribs and has a span length of 1.757 m. The wing was simulated using the multibody dynamics software Recurdyn® V9R3. Since the

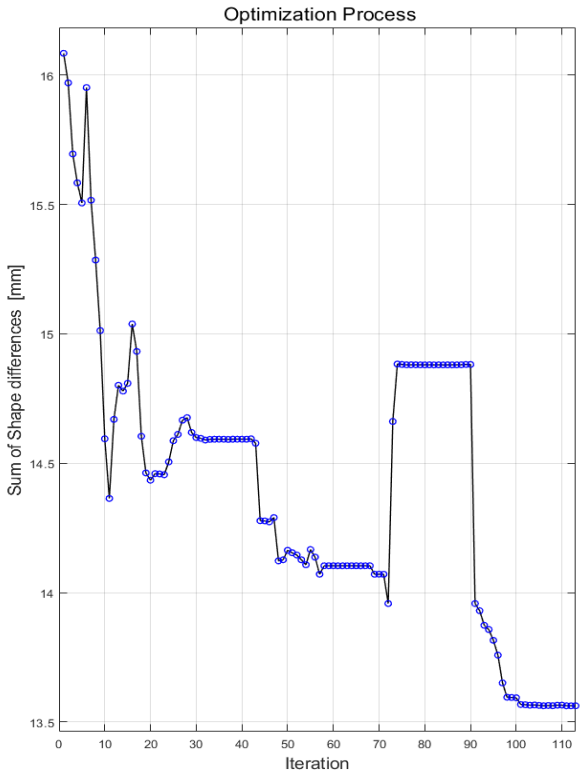

Fig. 9 The graph of the Shape differences' sum during the Optimization process

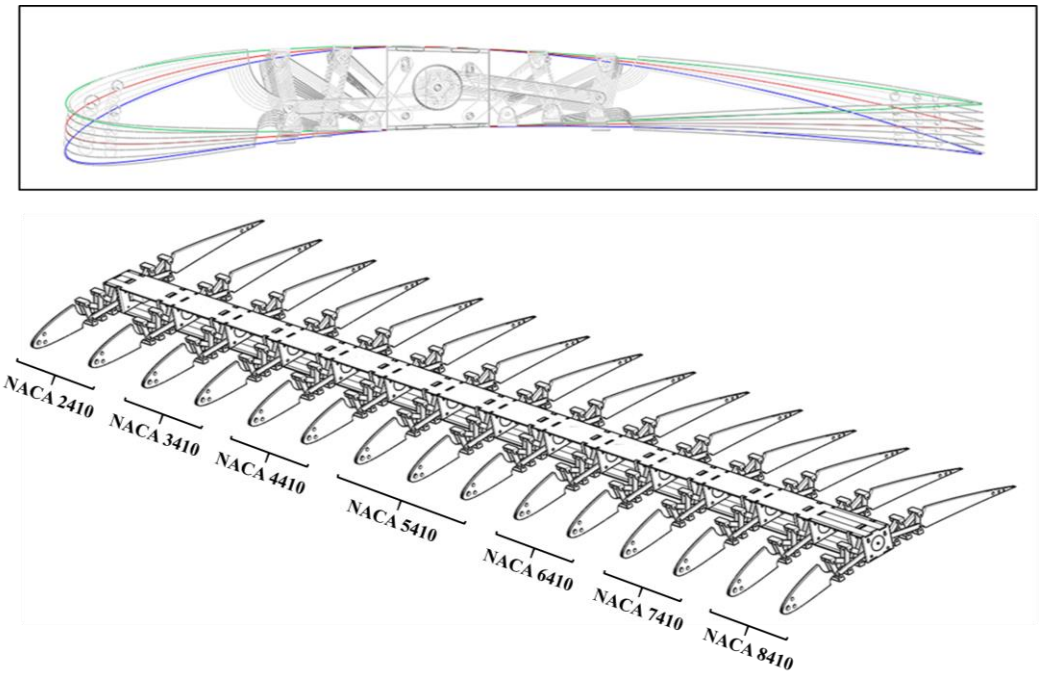

Fig. 10 Deformed into all target airfoils as a Twist morphing wing

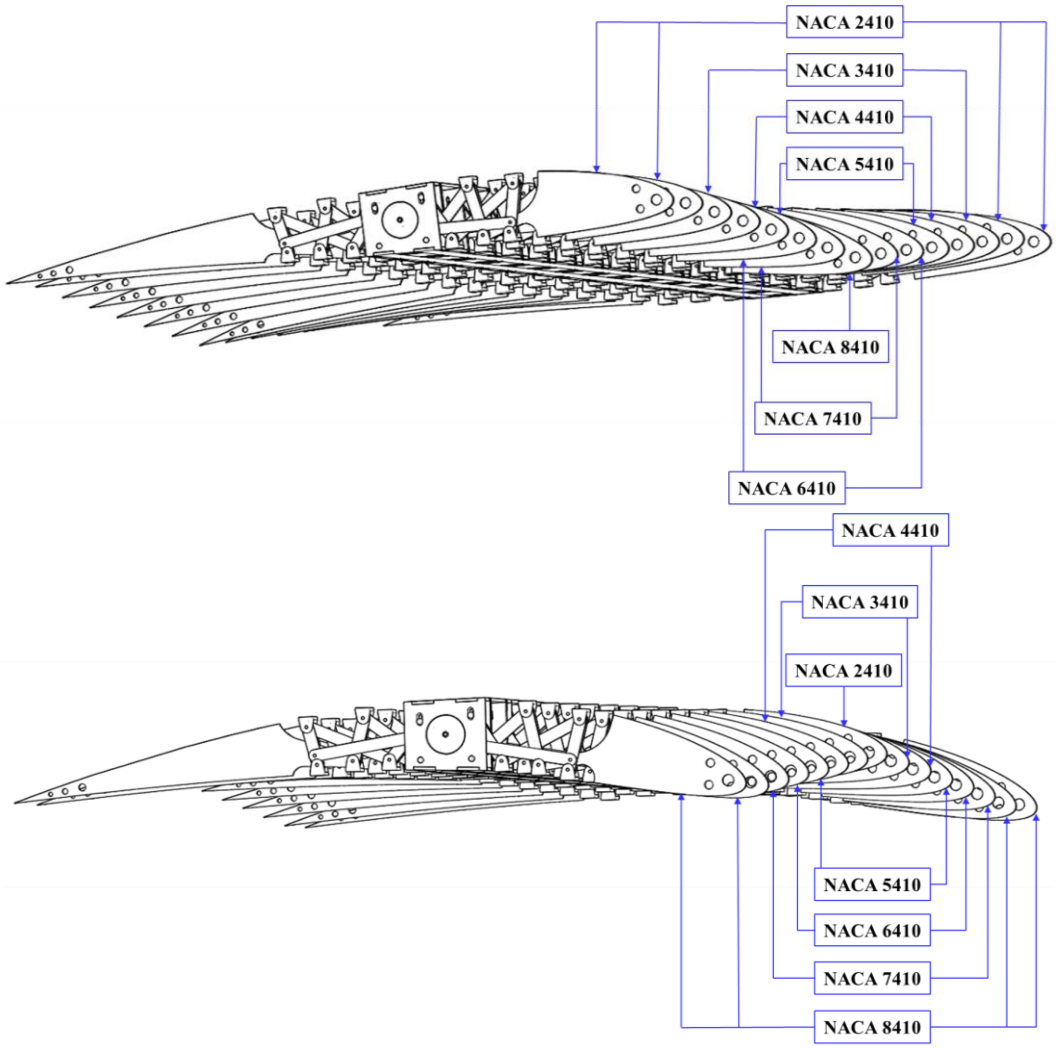

Fig. 11 The morphing wing deformed concave up and down

mechanism can be driven independently, a diverse combination of ribs that determine the overall shape of the morphing wing can be generated. In Fig. 10, the morphing wing is twisted by sequentially forming all target airfoil shapes. In other combinations, the morphing wing represents concave up and down by target shapes as shown in Fig. 11.

4. Manufacturing and performance evaluation of the Morphing structure

The designed morphing wing is manufactured by stainless wrench bolt, plywood and the rotating actuator. The actuator operating on a rib is a servo motor capable of generating torque up to 5.3 kg/cm-8.5 kg/cm. Because the morphing mechanism proposed in this paper designed was by focusing on the operability and manufacturability to shape desired airfoils, the geometries of scissors

members were determined with these considerations. The thickness and width of scissors members were set to the minimum value that can insert a rotary joint so that it can be manufactured lightly and operated. With these geometries, the drivability was confirmed by simulation using the multi dynamics software Recurdyn® V9R3.

The manufactured rib has 0.5 m length and has the same chord length as the designed rib model. Figs. 12 and 13 show the target airfoils' shapes (NACA 2410 and NACA 8410) indicated by thick green lines.

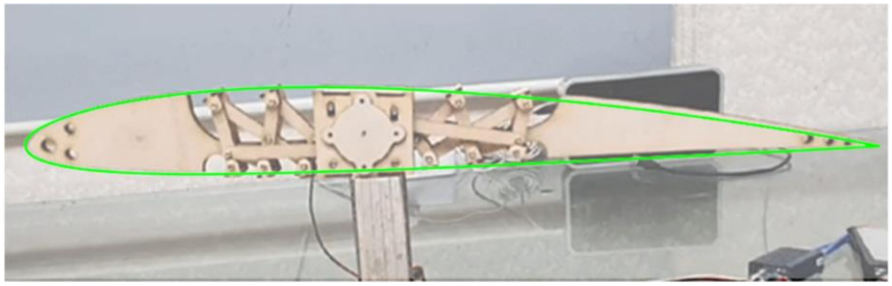

Fig. 12 The rib's shape for NACA 2410 with a target airfoil line

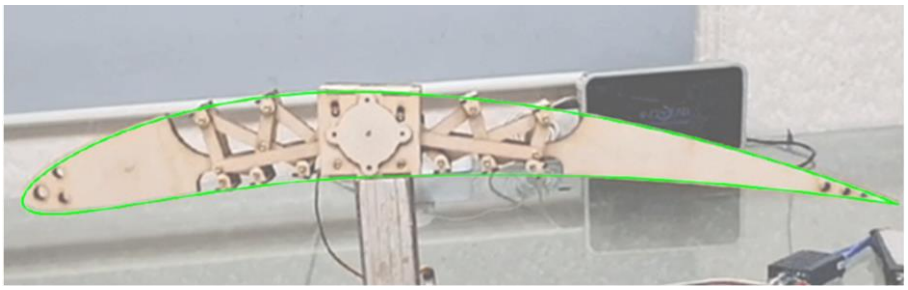

Fig. 13 The rib's shape for NACA 8410 with a target airfoil line

The designed morphing wing is manufactured with wing's span length of about 1.1m and ten ribs. The morphing wing is operated by inputting the angles through the controller. The controller sends a signal to the receiver, and the receiver is connected to the actuator to transmit the signal. Power is connected to the receiver. Futaba T18SZ was used for the controller. The motor was D89MW and the receiver was R7008SB. The operation configuration is depicted in Fig. 14, along with the morphing wing embodying the maximally twisted shapes.

5. Conclusions

This paper proposed a novel camber morphing wing mechanism with a new design methodology and the deployable scissor structure. The rib can form the targeted airfoil shapes with different cambers and constant chord lengths with the morphing mechanism. The wing comprised of the ribs can form various configurations by changing the camber.

A mathematical modeling and optimization processes were developed to design the internal

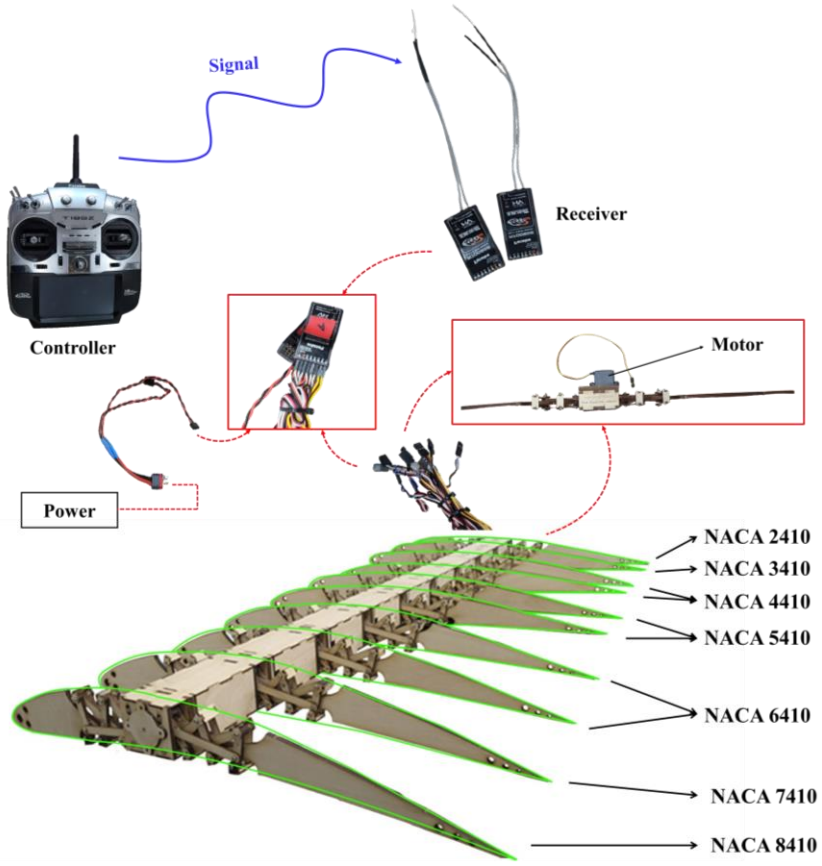

Fig. 14 Morphing wing operation process and manufactured wing deformed as twist morphing wing

mechanism that implements the targeted shapes. The lengths of the deployable scissors structure are determined through the optimization processes of minimizing the differences between the created shape and the target shape. The proposed design methodology can also determine any targeted shapes. The rib has one servo motor inside the spar, which is controlled by one variable: angle. Having one control variable is a considerable advantage since operating becomes much simplified. The morphing wing consisting of N ribs can be entirely operated with N control variables. Moreover, these ribs are operating independently. Therefore, the ribs' shapes can be combined in various ways depending on the requirement, and the wing can form diverse contours. Following the simulation by Recurdyn® V9R3, the rib and the wing were manufactured and operated successfully.

As the wing structure was performed successfully, the skin to cover the wing will be planned to be designed and fabricated. Since the wing shape changes, the skin should follow the wing shape by using a suitable material or a structural method for deformation. Therefore, the research for skin material and the morphing wing operation considering the effects of the aerodynamic pressure and the stiffness of the skin will be studied in the future. Also, the optimization process can be conducted by adding design variables such as the number of ribs according to the span, the distance between ribs, the number of desirable airfoils, etc. to existing design variables that determine the shape.

Acknowledgments

This research is based upon work supported by the Air Force Office of Scientific Research under award number FA2386-17-1-4081 and the Institute of Engineering Research at Seoul National University. The authors are grateful for their supports.

References

Abdulrahim, M. (2005), "Flight performance characteristics of a biologically-inspired morphing aircraft", *43rd AIAA Aerospace Sciences Meeting and Exhibit*, 345, January.

Abdulrahim, M. and Lind, R. (2004), "Flight testing and response characteristics of a variable gull-wing morphing aircraft", *AIAA Guidance, Navigation, and Control Conference and Exhibit*, 5113. August.

Ajaj, R.M., Flores, E.S., Friswell, M.I., Allegri, G., Woods, B.K.S., Isikveren, A.T. and Dettmer, W.G. (2013), "The Zigzag wingbox for a span morphing wing", *Aerosp. Sci. Technol.*, **28**(1), 364-375. https://doi.org/10.1016/j.ast.2012.12.002.

Ajaj, R.M., Friswell, M.I., Bourchak, M. and Harasani, W. (2016), "Span morphing using the GNATSpar wing", *Aerosp. Sci. Technol.*, **53**, 38-46. https://doi.org/10.1016/j.ast.2016.03.009.

Andersen, G., Cowan, D. and Piatak, D. (2007), "Aeroelastic modeling, analysis and testing of a morphing wing structure", *48th AIAA/ASME/ASCE/AHS/ASC Structures, Structural Dynamics, and Materials Conference*, 1734, April.

Barbarino, S., Bilgen, O., Ajaj, R.M., Friswell, M.I. and Inman, D.J. (2011), "A review of Morphing aircraft", *J. Intel. Mater. Syst. Struct.*, **22**(9), 823-877. https://doi.org/10.1177/1045389X11414084.

Bourdin, P., Gatto, A. and Friswell, M.I. (2008), "Aircraft control via variable cant-angle winglets", *J. Aircraft*, **45**(2), 414-423. https://doi.org/10.2514/1.27720.

Cuji, E. and Garcia, E. (2008), "Aircraft dynamics for symmetric and asymmetric V-shape Morphing wings", *Smart Materials, Adaptive Structures and Intelligent Systems*, Vol. 43321, 579-588, January.

Dale, A., Cooper, J.E. and Mosquera, A. (2013), "Adaptive Camber-Morphing wing using 0-? Honeycomb", *54th AIAA/ASME/ASCE/AHS/ASC Structures, Structural Dynamics, and Materials Conference*, 1510.

Detrick, M. and Washington, G. (2007), "Modeling and design of a morphing wing for micro unmanned aerial vehicles via active twist", *48th AIAA/ASME/ASCE/AHS/ASC Structures, Structural Dynamics, and Materials Conference*, 1788, April.

Dimino, I., Ciminello, M., Gratias, A., Schueller, M. and Pecora, R. (2017), "Control system design for a morphing wing trailing edge", *Smart Structures and Materials*, 175-193, Springer, Cham.

Elzey, D.M., Sofla, A.Y.N. and Wadley, H.N. (2003), "A bio-inspired high-authority actuator for shape morphing structures", *Smart Sstructures and Materials 2003: Active Materials: Behavior and Mechanics*, Vol. 5053, 92-100, August.

de Marmier, P. and Wereley, N. (2003), "Control of sweep using pneumatic actuators to morph wings of small scale UAVs", *44th AIAA/ASME/ASCE/AHS/ASC Structures, Structural Dynamics, and Materials Conference*, 1802.

De Temmerman, N. (2007), "Design and analysis of deployable bar structures for mobile architectural applications", Ph.D. Dissertation, Vrije Universiteit Brussel, Brussels, Belgium.

Finistauri, A.D. and Xi, F.J. (2009), "Type synthesis and kinematics of a modular variable geometry truss mechanism for aircraft wing morphing", *2009 ASME/IFToMM International Conference on Reconfigurable Mechanisms and Robots*, 478-485.

Fenci, G.E. and Currie, N.G. (2017), "Deployable structures classification: A review", *Int. J. Space Struct.*, **32**(2), 112-130. https://doi.org/10.1177/0266351117711290.

Joo, J.J., Marks, C.R., Zientarski, L. and Culler, A.J. (2015), "Variable camber compliant wing-design 23rd AIAA", AHS Adaptive Structures Conference.

Kimaru, J. and Bouferrouk, A. (2017), "Design, manufacture and test of a camber morphing wing using MFC

actuated mart rib", *2017 8th International Conference on Mechanical and Aerospace Engineering (ICMAE)*, 791-796, July.
Langbecker, T. (1999), "Kinematic analysis of deployable scissor structures", *Int. J. Space Struct.*, **14**(1), 1-15. https://doi.org/10.1260/0266351991494650.
Majji, M., Rediniotis, O. and Junkins, J. (2007), "Design of a morphing wing: modeling and experiments", *AIAA Atmospheric Flight Mechanics Conference and Exhibit*, 6310, August.
Marks, C.R., Zientarski, L., Culler, A.J., Hagen, B., Smyers, B.M. and Joo, J.J. (2015), "Variable camber compliant wing-wind tunnel testing", *23rd AIAA/AHS Adaptive Structures Conference*, 1051.
Marques, M., Gamboa, P. and Andrade, E. (2009), "Design and testing of a variable camber flap for improved efficiency", *The Applied Vehicle Technology Panel Symposium (AVT-168)*, April.
Mestrinho, J., Gamboa, P. and Santos, P. (2011), "Design optimization of a variable-span morphing wing for a small UAV", *52nd AIAA/ASME/ASCE/AHS/ASC Structures, Structural Dynamics and Materials Conference 19th AIAA/ASME/AHS Adaptive Structures Conference 13t*, 2025.
Monner, H., Kintscher, M., Lorkowski, T. and Storm, S. (2009), "Design of a smart droop nose as leading edge high lift system for transportation aircrafts", *50th AIAA/ASME/ASCE/AHS/ASC Structures, Structural Dynamics, and Materials Conference 17th AIAA/ASME/AHS Adaptive Structures Conference 11th AIAA No*, 2128, May.
Pagani, A., Zappino, E., de Miguel, A.G., Martilla, V. and Carrera, E. (2019), "Full field strain measurements of composite wing by digital image correlation", *Adv. Aircraft Spacecraft Sci.*, **6**(1), 69-86. https://doi.org/10.12989/aas.2019.6.1.069.
Prabhakar, N., Prazenica, R.J. and Gudmundsson, S. (2015), "Dynamic analysis of a variable-span, variable-sweep morphing UAV", *2015 IEEE Aerospace Conference*, 1-12, March.
Raither, W., Heymanns, M., Bergamini, A. and Ermanni, P. (2013), "Morphing wing structure with controllable twist based on adaptive bending–twist coupling", *Smart Mater. Struct.*, **22**(6), 065017. https://doi.org/10.1088/0964-1726/22/6/065017.
Rivero, A.E., Weaver, P.M., Cooper, J.E. and Woods, B.K. (2017), "Progress on the design, analysis and experimental testing of a composite fish bone active camber Morphing wing", *ICAST 2017: 28th International Conference on Adaptive Structures and Technologies*, 1-11, October.
Rivero, A.E., Weaver, P.M., Cooper, J.E. and Woods, B.K. (2018), "Parametric structural modelling of fish bone active camber morphing aerofoils", *J. Intel. Mater Syst. Struct.*, **29**(9), 2008-2026. https://doi.org/10.1177/1045389X18758182.
Roovers, K. and De Temmerman, N. (2017), "Deployable scissor grids consisting of translational units", *Int. J. Solid. Struct.*, **121**, 45-61. https://doi.org/10.1016/j.ijsolstr.2017.05.015.
Seow, A.K., Liu, Y. and Yeo, W.K. (2008), "Shape memory alloy as actuator to deflect a wing flap", *49th AIAA/ASME/ASCE/AHS/ASC Structures, Structural Dynamics, and Materials Conference, 16th AIAA/ASME/AHS Adaptive Structures Conference, 10th AIAA Non-Deterministic Approaches Conference, 9th AIAA Gossamer Spacecraft Forum, 4th AIAA Multidisciplinary Design Optimization Specialists Conference*, 1704.
Sofla, A.Y.N., Meguid, S.A., Tan, K.T. and Yeo, W.K. (2010), "Shape morphing of aircraft wing: Status and challenges", *Mater. Des.*, **31**(3), 1284-1292. https://doi.org/10.1016/j.matdes.2009.09.011.
Tarabi, A., Ghasemloo, S. and Mani, M. (2016), "Experimental investigation of a variable-span morphing wing model for an unmanned aerial vehicle", *J. Brazil. Soc. Mech. Sci. Eng.*, **38**(7), 1833-1841. https://doi.org/10.1007/s40430-015-0405-6.
Vocke III, R.D., Kothera, C.S., Woods, B.K. and Wereley, N.M. (2011), "Development and testing of a span-extending morphing wing", *J. Intel. Mater. Syst. Struct.*, **22**(9), 879-890. https://doi.org/10.1177/1045389X11411121.
Vos, R., Gürdal, Z. and Abdalla, M. (2010), "Mechanism for warp-controlled twist of a morphing wing", *J. Aircraft*, **47**(2), 450-457. https://doi.org/10.2514/1.39328.
Wlezien, R.W., Horner, G.C., McGowan, A.M.R., Padula, S.L., Scott, M.A., Silcox, R.J. and Harrison, J.S. (1998), "Aircraft morphing program", *Smart Structures and Materials 1998: Industrial and Commercial Applications of Smart Structures Technologies*, Vol. 3326, 176-187.

Yokozeki, T., Sugiura, A. and Hirano, Y. (2014), "Development and wind tunnel test of variable camber morphing wing", *22nd AIAA/ASME/AHS Adaptive Structures Conference*, 1261.

Yokozeki, T., Sugiura, A. and Hirano, Y. (2014a), "Development of variable camber morphing airfoil using corrugated structure", *J. Aircraft*, **51**(3), 1023-1029. https://doi.org/10.2514/1.C032573.

Zhang, J., Shaw, A.D., Wang, C., Gu, H., Amoozgar, M., Friswell, M.I. and Woods, B.K. (2021), "Aeroelastic model and analysis of an active camber morphing wing", *Aerosp. Sci. Technol.*, **111**, 106534. https://doi.org/10.1016/j.ast.2021.106534.

Zhao, J.S., Chu, F. and Feng, Z.J. (2009), "The mechanism theory and application of deployable structures based on SLE", *Mech. Mach. Theory*, **44**(2), 324-335. https://doi.org/10.1016/j.mechmachtheory.2008.03.014.

CC